Available online at www.sciencedirect.com
SCIENCE DIRECT
Composites: Part A 37 (2006) 430–437
composites Part A: applied science and manufacturing
www.elsevier.com/locate/compositesa

Compressive characteristics of A356/fly ash cenosphere composites synthesized by pressure infiltration technique

P.K. Rohatgi[a], J.K. Kim[a], N. Gupta[b,*], Simon Alaraj[c,1], A. Daoud[d]

[a]Materials Department, University of Wisconsin, Milwaukee, 3200 N. Cramer St, Milwaukee, WI 53211, USA
[b]Mechanical, Aerospace and Manufacturing Engineering Department, Polytechnic University, Brooklyn, NY 11201, USA
[c]Mechanical Engineering Department, Birzeit University, Birzeit, Palestine
[d]Composite Material Lab., Central Metallurgical Research and Development Institute (CMRDI), P.O. Box 87, Helwan, Cairo, Egypt

Received 20 February 2005; revised 22 May 2005; accepted 22 May 2005

Abstract

Loose beds of hollow fly ash particles (cenospheres) were pressure infiltrated with A356 alloy melt to fabricate metal-matrix syntactic foam, using applied pressure up to 275 kPa. The volume fractions of cenospheres in the composites were in the range of 20–65%. The processing variables included melt temperature, gas pressure and particles size of fly ash. The effect of these processing variables on the microstructure and compressive properties of the synthesized composites is characterized. Compressive tests performed on these metal-matrix composites containing different volume fractions of hollow fly ash particles showed that their yield stress, Young's modulus, and plateau stress increase with an increase in the density. Variations in the compressive properties of the composites in the present study were compared with other foam materials.

Keywords: A. Foams; A. Metal-matrix composites; A. Particle reinforcement; D. Mechanical testing

1. Introduction

The pressure infiltration technique is capable of synthesizing Metal-Matrix Composite (MMC) with high volume fraction and uniform distribution of the particles in the matrix [1]. Other techniques such as stir mixing can synthesize MMCs having only up to 30% particles by volume and are at a disadvantage compared to the pressure infiltration technique. The pressure infiltration technique is used for the fabrication of MMCs containing fibrous or particulate reinforcement [2–5]. Recently, hollow spherical particles, composed of carbon, glass, alumina and other materials, have been incorporated in metallic and polymeric matrices to make syntactic foam composites [6–10]. Since, the hollow particles have lower density than the matrix, the density of the resulting composite is lower then that of the matrix. Such an approach permits the design of lightweight and stiff components. The ceramic particle filled syntactic foams have excellent thermal insulation properties and low thermal expansion coefficient due to a significant volume fraction of ceramic phase in the structure. Syntactic foams are attractive materials for energy absorbing applications due to their large compressive strains. In addition, these foam materials are likely to possess unique properties such as high energy damping capacity [11].

In this study, syntactic foams are fabricated by infiltrating loose beds of hollow fly ash particles, called cenospheres, with A356 alloy melt. Cenospheres are classified based on their size and density to obtain appropriate properties in resulting composites. Some studies on the synthesis of cenosphere filled syntactic foams can be found published in the literature. A variety of matrix materials are used in such composites including metals and polymers. However, a comprehensive investigation of the effect of various processing parameters on the microstructures and compressive properties of syntactic foams is necessary in view of their increasing demand in the present times.

The processing parameters that were varied in this study are applied gas pressure, temperature, cenosphere volume

* Corresponding author. Tel.: +1 718 260 3080; fax: +1 718 260 3532.
E-mail address: ngupta@poly.edu (N. Gupta).
[1] Present address: University of Wisconsin, Milwaukee, WI, USA.

1359-835X/$ - see front matter © 2005 Elsevier Ltd. All rights reserved.
doi:10.1016/j.compositesa.2005.05.047

fraction and cenosphere size. Compression tests are carried out for specimens fabricated under each condition to characterize the compression properties, including the 0.2% yield stress, plateau stress, and compressive strength. The compressive properties of the composites are related to various processing and material parameters.

2. Materials and experimental procedures

2.1. Materials

A356 is a cast aluminum alloy that has Si 7.0%, Fe 0.2% Cu 0.2%, Mg 0.35% and Mn 0.10% by weight. This alloy has good weldability, corrosion resistance and resistance to hot cracking and solidification shrinkage [12].

The fly ash particles are alumino-silicate based ceramic particles, which can be either solid or hollow. The hollow fly ash particles are called cenospheres and are separated from solid particles by using flotation methods. These particles used as fillers in the present work have the major chemical constituents as given in Table 1. The hollow particles of different sizes may have the same density because of a difference in their wall thickness. The true particle density of fly ash cenospheres used in the present experiments is around 700 kg/m^3, measured by the gas expansion method, the wall thickness varies over a range of 4–12 μm and diameters vary from 45 to 250 μm. The density of the ceramic material forming cenospheres is around 2650 kg/m^3. However, the lower density of cenospheres is due to the presence of a cavity within these particles.

2.2. Specimen preparation through the pressure infiltration process

The fly ash cenospheres are separated into four groups based on their diameter using a set of sieves. These size groups are 45–75, 75–106, 106–150, and 150–250 μm. To make composites having high volume fraction of particles (>57%), fly ash is loosely packed into a borosilicate glass tubes coated with a ceramic layer of ZrO_2 to prevent reaction with molten A356 alloy and gently tapped for 5 min. Each tube was 230 mm long with an outer diameter of 18 mm and an internal diameter of 16 mm. To fabricate lower fly ash volume fraction (<35%) composites a mixture of fly ash and A356 alloy powder was prepared taking their appropriate volume fractions and filled into the hollow tubes. Tubes containing fly ash or fly ash-A356 powder mixture were placed into an oven at 250 °C for 1 h for drying.

The pressure infiltration equipment used in fabricating the composites is shown in Fig. 1. This equipment consists of a stainless steel chamber, which contains a resistance heater. Inside the chamber is a graphite coated crucible that rests on a refractory base. A356 alloys is placed in this crucible and melted; the temperature of the melt is raised to either 720 or 800 °C as per the desired processing conditions. The preheated borosilicate tubes containing packed cenospheres are attached to the heater lid through a Swaglock compression fitting, and the lid is placed onto the heater. The lid is then held in place through a customized locking system. Once the system is sealed, the pressure is applied to the chamber using nitrogen gas to achieve a pre-decided value and maintained at that level for 2 min. The pressure causes the molten alloy to rise into the cenosphere filled glass tube. Two minutes was considered sufficient time for the liquid alloy to infiltrate the interstitial spaces between cenospheres and form the composite. At the end of the process the pressure is released and the composite is removed.

Nine types of composites were fabricated using a combination of different cenosphere sizes, volume fractions, infiltration pressures and processing temperatures as per the details presented in Table 2. In addition, the base alloy A356 was cast without reinforcements to obtain properties of the matrix alloy.

The bottom 50 mm was removed from all cast syntactic MMCs because these portions of the tube extends below the surface of the A356 melts in the crucible. The top portion of some MMCs was also cut because they exhibit incomplete filling due to freeze choking of the melt coming in contact with fly ash cenospheres which are at a comparatively lower temperature. Specimens were sectioned from the remaining portions using Enco water cooled cutoff wheel and were used for microstructural analysis and measuring the density, the hardness, and the compressive strength.

2.3. Compression test

To evaluate the influence of cenosphere particles on the compressive properties of the composites, the 0.2% yield stress, the plateau stress, and the compressive strength were measured in accordance with standard ASTM E 9-89A. Specimens having height/diameter ratio (aspect ratio) of two were cut and their ends were turned to ensure the parallelism. The specimens were then compressed in a computer controlled Universal Static Compression Tester at the crosshead speed of 1.3 mm/min. The load–displacement

Table 1
Typical chemical composition of fly ash in weight percent

Al_2O_3	SiO_2	CaO	Fe_2O_3	MgO	K_2O	Na_2O	TiO_2	SO_3	LOI[a]
15–30	30–70	1–5	10–20	0–2	1–5	0–2	0–2	0–2	0–10

[a] LOI, loss of ignition.

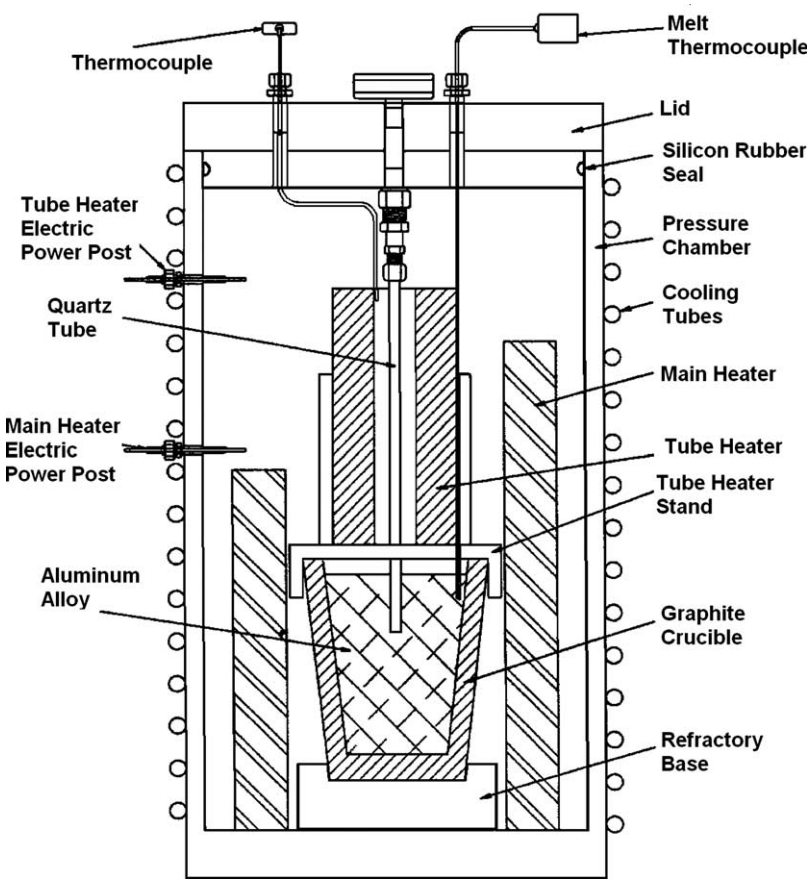

Fig. 1. Pressure infiltration experimental set-up.

data collected was then used to calculate and plot stress vs. strain curves.

2.4. Microstructure observation

Metallographic specimens are taken from the top, the middle, and the bottom of all infiltrated MMCs. The infiltrated specimens were cut transverse to the direction of infiltration at these locations. Standard polishing procedures are followed using SiC grinding papers to 600 grit. Final polishing is carried out on a micropolishing cloth with a 0.05 μm SiO_2 slurry. Specimens are then polished to observe the microstructures using optical microscope (Olympus/BH2-UMA) and Scanning electron microscope (SEM).

3. Results

3.1. Microstructure analysis and void content measurement

The microstructure of the fabricated specimens contains porosity in two forms. The first form of porosity has close

Table 2
Details of various synthesized composites with their densities and void content

Composite no.	Fly ash size (μm)	Volume fraction (%)	Melt temperature (°C)	Pressure (kPa)	Measured density (kg/m^3)	Calculated density (kg/m^3)[a]	Void content %
1	75–106	65	720	205	1250	1379	9.3
2	106–150	65	720	205	1270	1379	7.9
3	150–250	65	720	205	1300	1379	5.7
4	150–250	57	800	140	1410	1534	8.1
5	150–250	57	800	205	1430	1534	6.8
6	150–250	57	800	275	1470	1534	4.2
7	150–250	35	800	275	1900	1961	3.1
8	150–250	25	800	275	2100	2155	2.6
9	150–250	20	800	275	2180	2252	3.2
10	A356	0	800	70	2640	–	–

[a] Calculated using rule of mixtures.

cell structure and is entirely contained within the cenospheres. This form of porosity has been deliberately introduced in the composite to produce a lightweight material. The second form of porosity is due to the incomplete infiltration that results from the low applied infiltration pressures employed here. This second form of porosity is not deliberately introduced, and hence a priori undesirable. We call in what follows this second form of porosity 'void content', and designate corresponding pores as 'voids'. The difference between theoretical and measured densities of the composites is used for the calculation of void content (V_v) in the composite as per Eq. (1) [13]

$$V_v = \frac{\rho_{ct} - \rho_{ce}}{\rho_{ct}} \quad (1)$$

where ρ_{ct} and ρ_{ce} are theoretical and measured density values of the fabricated composites. The theoretical densities of composites were calculated using Rule of Mixtures. The measured and theoretically calculated densities of all types of composites synthesized in this study are given in Table 2. The experimentally measured density of A356 alloy is also presented in Table 2, which is used in the Rule of Mixtures to calculate theoretical densities of composites.

The first composite is fabricated by infiltrating a bed of 75–106 μm size cenospheres at a pressure of 205 kPa at 720 °C. The microstructure of a specimen taken from this composite is shown in Fig. 2. It is observed that most of the cenospheres are uniformly distributed in the matrix. Some areas of incomplete infiltration (indicated by arrows), leading to voids, can be observed in the structure. Such regions are related to high capillary resistance near interparticle contact regions. Other researchers have also observed pores present near interparticle contact regions in many different MMC systems [14,15]. The values in Table 2 show that the first composite has 9.3% void content by volume and suggest that an applied pressure of 205 kPa at 720 °C is not high enough to infiltrate all interparticle spaces

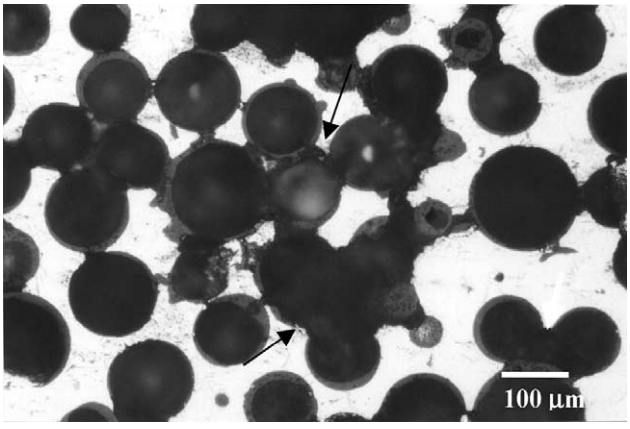

Fig. 2. Microstructure of A356–fly ash cenospheres syntactic foam, infiltrated at an applied pressure of 205 kPa with cenospheres size and volume fraction of 75–106 μm and 65%, respectively.

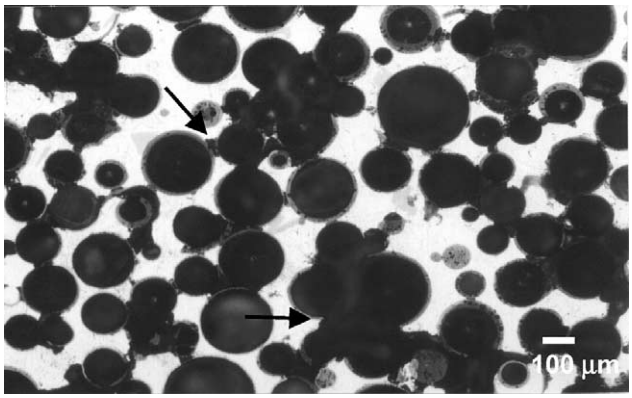

Fig. 3. Microstructure of A356–fly ash cenospheres syntactic foam, infiltrated at an applied pressure of 205 kPa with cenospheres size and volume fraction of 106–150 μm and 65%, respectively.

in 75–106 μm size cenospheres. Hence, larger size cenospheres, 106–150 μm, with the same infiltration pressure and melt temperature are used in the second composite.

The microstructure of the second type of syntactic composites is shown in Fig. 3. This composite is found to have 7.9% voids by volume, which is 1.4% lower than the previous composite having smaller size cenospheres. The interparticle spacing increases with the increase in particle size, when all other variables are kept unchanged. An increase in the interparticle spacing reduces the capillary resistance and results in lower porosity at the same infiltration pressure. This trend is confirmed when the third composite with 150–250 μm size particles is fabricated under the same processing conditions. The void content in these samples is calculated to be around 5.7% by volume as shown in Table 2, which is lower than the first two composites that have smaller size cenospheres.

To investigate the effect of infiltration pressure on the void content, composites 4–6 were fabricated using 150–250 μm size cenospheres, particle volume fraction of 57% and increased melt temperature of 800 °C while the pressure is varied from 140 to 275 kPa. Table 2 shows that as the pressure is increased from 140 to 205 and to 275 kPa the void content decreases from 8.1 to 6.8 and to 4.2%, respectively. The microstructure of a specimen of type 6 composite is shown in Fig. 4, where voids between cenospheres are marked by arrows. The pressure was not increased further in this study because cenosphere fracture may take place at higher pressures. Some dark colored arcs visible in the lower part of the microstructure in Fig. 4 appear to be the broken cenospheres infiltrated by the melt. Under the present infiltration conditions the damage to microballoons does not seem to be substantial but any further increase in the infiltration pressure may lead to higher volume fraction of fractured cenospheres, which is undesirable.

It can be seen from Figs. 2–4 that the pores are generally present at interparticle contact regions, where a high applied pressure is required for the melt to infiltrate. The melt flow

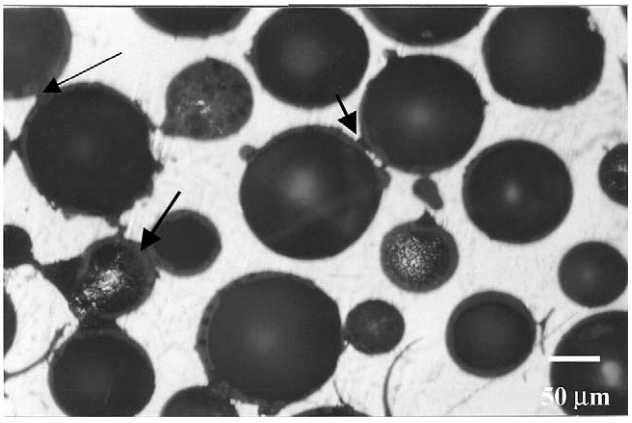

Fig. 4. Microstructure of A356–fly ash cenospheres syntactic foam, infiltrated at an applied pressure of 275 kPa with cenospheres size and volume fraction of 150–250 µm and 57%, respectively.

in the bed becomes easier at a higher melt temperature due to a lower viscosity of the melt, thereby resulting in a higher density of the composite and a lower void content.

In composites 7–9, A356 powder and fly ash cenospheres with particle size range of 150–250 µm were mixed prior to infiltration to maintain lower cenosphere volume fractions, 35, 25 and 20%, in the fabricated syntactic foams. These composites are infiltrated at 275 kPa pressure and 800 °C temperature. It can be noted from Table 2 that the void content for these composites is around 3% by volume, which is lower than all of the previous composites. The approach of mixing A356 powder with cenospheres, which melts during the infiltration process, may be a factor in the reduced porosity apart from having low capillary resistance due to the low cenosphere volume fraction.

3.2. Compressive properties

Compressive properties of the synthesized MMCs can be understood by studying the stress–strain curves. Table 3 shows the 0.2% yield strengths and Young's moduli for all types of composites synthesized in this study. Fig. 5 shows the stress–strain curve for the A356 matrix alloy and for the composites types 7–9. It is shown that as the volume fraction of the particles increases from 20 to 35%, the corresponding

Table 3
Measured compressive properties of syntactic composites and matrix alloy

Composite no.	Fly ash size (µm)	0.2% Yield strength (MPa)	Young's modulus (MPa)
1	75–106	9	1274
2	106–150	17	2562
3	150–250	34	3111
4	150–250	25	3119
5	150–250	30	3548
6	150–250	49	3768
7	150–250	64	3826
8	150–250	73	4125
9	150–250	75	4355

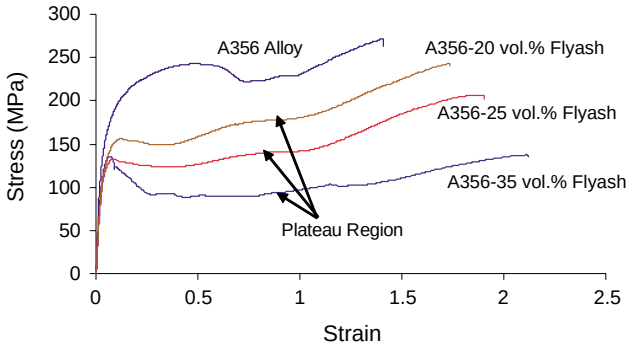

Fig. 5. Stress–strain curves for pure A356 alloy and A356–fly ash cenosphere syntactic foam containing 20, 25, and 35 vol.% cenospheres with size of 150–250 µm, infiltrated at 275 kPa pressure.

compressive yield strength decreases from 75 to 64 MPa. Generally, hollow particles have strength lower then the matrix strength, therefore, a decrease in compressive strength of the composite is observed with increase in cenosphere volume fraction.

The stress–strain curves in Fig. 6 are for the composites containing 65 vol.% of cenospheres of different size (composites 1–3 in Table 2). The figure shows that the yield strength decreases from 34 to 9 MPa as the cenosphere size decreases from 150–250 to 75–105 µm. The higher void content in composites containing smaller size cenospheres may be responsible for this type of trend.

The stress–strain curves for composites 4–6 are shown in Fig. 7. These composites have the same size cenospheres (150–250 µm) but are synthesized at different infiltration pressures as given in Table 2. It is observed that the compressive yield strength is higher for composites synthesized at higher infiltration pressures. This observation is also related to a lower void content in the matrix at the higher applied pressure. The composite infiltrated at 140 kPa have 8.1 vol.% void content which is almost twice the void volume fraction in the composite infiltrated at 275 kPa.

There is an additional factor related to the cenosphere size and wall thickness that can cause some variations in

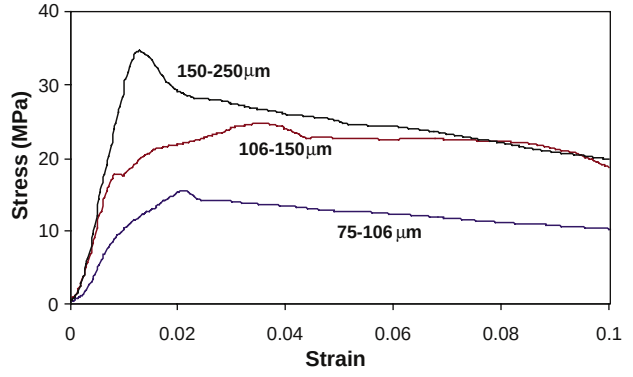

Fig. 6. Stress–strain curves for A356–fly ash cenosphere syntactic foam containing 65 vol.% fly ash cenosphere particles of different sizes.

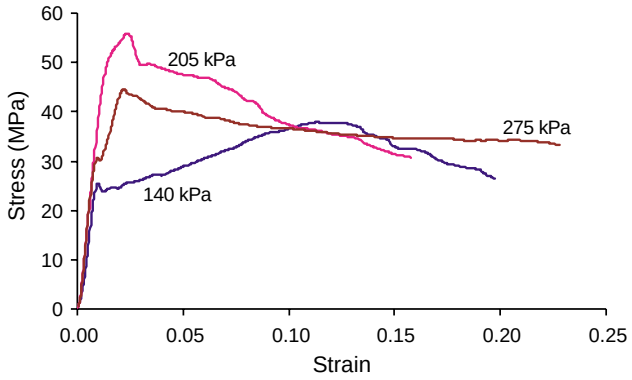

Fig. 7. Stress–strain curves for A356–fly ash cenosphere (size 150–250 μm) composites infiltrated at different applied pressures.

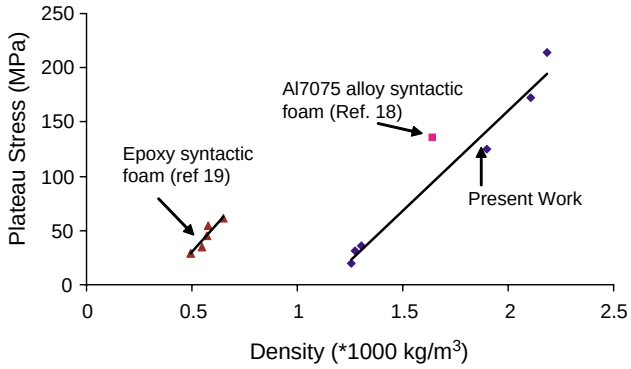

Fig. 8. Variation in plateau stress with density.

the compressive strength and modulus of the composites. Fly ash cenospheres have porosity entrapped in their walls [16], which changes with particle size and wall thickness. It should also be recognized that with a variation in the cenosphere size, the porosity of the wall of cenospheres can also change. Thicker walled or larger diameter cenospheres have higher probability of having entrapped porosity in their walls. This porosity would affect the mechanical properties of the cenospheres and reflect in the mechanical properties of the composite.

4. Discussion

Al–fly ash composites are found studied in the published literature for interfacial reactions between the molten Al alloy and the constituents of fly ash. It is observed that SiO_2 and Fe_2O_3, Fe_3O_4 and Mullite present in the fly ash readily react with Al and form a network of α-Al_2O_3 particles surrounded by Al or Si. A detailed TEM investigation of these interfacial phases and their structures is carried out by Sobczak et al. [17]. The interfacial reactions and the products define the interfacial strength between the particles and the matrix alloy and affect the properties of the composites. However, the effect of interfacial strength is more prominent on tensile and flexural properties. In compressive tests, the fracture mode of the syntactic foams is observed to be the crushing of cenospheres followed by the collapse of the metal-matrix surrounding it, leading to the structural densification. Hence, the breakage of interfacial bonds may not significantly influence the compressive strength.

Typical compressive stress–strain curves for A356/hollow fly ash composites and A356 alloy are shown in Fig. 5. Compressive stress–strain curves for the composites containing hollow particles show a linear elastic region followed by a plateau (possibly representing collapse of hollow particles), and then increase in stress, representing densification of foam. Fig. 8 shows that the plateau stress increases with increasing density of the composite. The plateau stress of a similar A7075-T6 syntactic foam made by pressure infiltration of fly ash cenosphere [18] is compared with that of the composite made in the present study, showing that the former has a higher plateau stress than the latter. This could be related to the higher strength of the matrix alloy of A7075 (about 350 MPa) compared to that of A356 alloy (about 240 MPa), which is used in the present study. Plateau stress of some polymeric syntactic foams made of epoxy resin and glass microballoons are also shown in Fig. 8 for comparison [19]. Although polymeric syntactic foams have much lower density compared to A356–fly ash syntactic composites for the same strength, their applications are limited because their strength can rarely exceed 100 MPa and the service temperature range is also much lower compared to metal-matrix syntactic foams.

Since, the stress plateau is possibly associated with the collapse of hollow particles, the continued compression will cause the cavity to be filled by the collapsing walls of cenospheres and surrounding matrix materials. A microstructure of crushed cenospheres in an Al-alloy matrix is shown in Fig. 9. Cenospheres were completely crushed under compressive stress. The crushing process of cenospheres enhances the energy absorption capabilities of syntactic foams leading to better damage tolerance of these materials. An increase in the plateau stress and a decrease in the range of strain at the plateau stress are observed in Fig. 5 as the cenosphere volume fraction decreases in the syntactic foams. This tendency is also observed in many different foam materials, including polyurethane, polyethylene, metallic foams and polymeric syntactic foams [20–22].

The plateau stress represents the onset of the mechanical instability of composites containing hollow particles, and therefore, is one of the important design factors for cushions or impact mitigation. The plateau strain at which the densification of particles is completed is also important, since it is influenced by the energy absorbed in crushing of cenospheres. It can be observed from Figs. 5–7 that a larger plateau strain range is likely to be attained by increasing volume fraction of hollow particles in the matrix. According to Hartmann et al. [6], the plateau stress increases with increasing the wall thickness of hollow

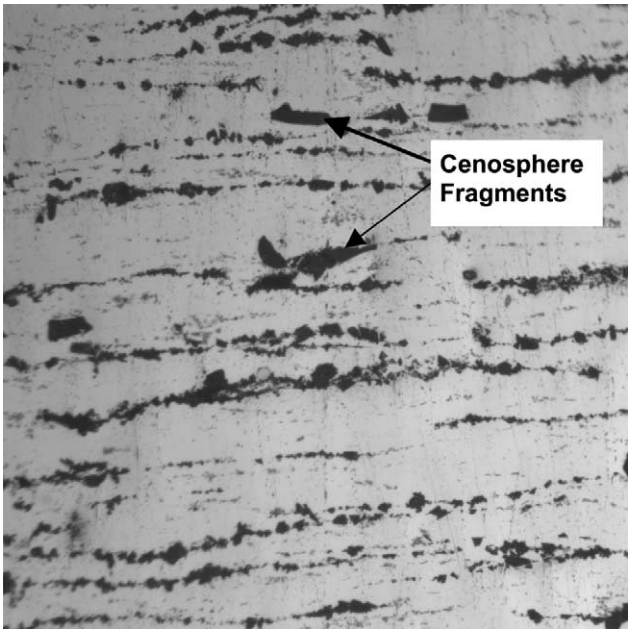

Fig. 9. A micrograph showing general appearance of the microstructure of A356–fly ash composite after compression test. Crushed fly ash particles can be observed in the microstructure.

particles. Similar observations have been made in glass microballoon filled polymeric syntactic foams also [19,23]. This is related to the fact that the load carrying capabilities of hollow particles increase with increased wall thickness. Therefore, composites with higher energy absorption may be obtained by increasing the volume fraction of cenospheres in the matrix and by increasing the wall thickness of cenospheres.

The Young's modulus of foams is primarily related to their density; for syntactic foams the wall material and wall thickness of hollow particles considerably influence the mechanical properties. When the Young's modulus of ceramic filler particles is higher than that of the metallic matrix alloy, the syntactic composite is expected to have a higher modulus than that of foam materials having only pores without particles. Nagal et al. [24] have also made similar observations.

There have been extensive investigations of open cell foams [25–27], for which there are validated scaling relations between density, cell morphology and cell wall properties. When foam is compressed, it initially deforms in a linear-elastic manner, then reaches a plateau of deformation at almost constant stress, and finally exhibits a region of densification as the cell walls crush together. This tendency is similar to that in composites containing hollow particles shown in Fig. 4.

In composites containing hollow particles, the hollow spaces inside the particles act as pores, which absorb energy when crushed. In such composites, the cell morphology is primarily controlled by the distribution and packing of hollow particles. High packing density of particles and a narrow range of particle size will provide more uniform cell

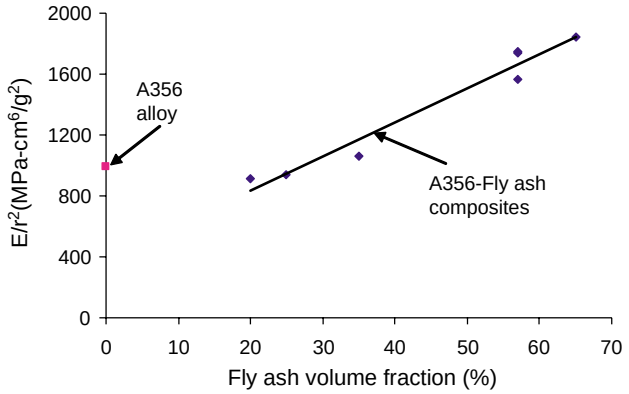

Fig. 10. Variation of the ratio of Young's modulus to density of the sample with the volume fraction of cenosphere particles. The data for all specimens containing 150–250 μm are shown in the figure.

morphology than the foams made using foaming agents in melts. From thermodynamic point of view, pores in the melt tend to decrease their numbers and increase their size. Hence, the pressure infiltration of hollow particle beds presents an advantage since it leads to generation of relatively uniform cell walls. This leads to more uniform and improved mechanical properties in contrast to the properties obtained in foam materials made using foaming agents.

The effectiveness of a composite containing hollow particles is likely to be evaluated in terms of the bending and the axial stiffness. The mass of a beam of a given bending stiffness can be minimized by selecting the material with the maximum value of E/ρ^2 for axial stiffness. Fig. 10 shows the variation of E/ρ^2 for the composites having 150–250 μm size cenospheres plotted against the volume fraction of cenosphere particles. The maximum value of E/ρ^2 for the composite up to 65% by volume is around 1850 MPa cm^6 g^{-2}. This figure shows that the values of E/ρ^2 increase with increased volume fraction of cenospheres, and the values of E/ρ^2 for fly ash containing composites are higher than those for A356 alloy. In view of this, higher volume fractions of cenospheres are expected to allow the synthesis of materials with higher values of E/ρ^2.

5. Conclusions

1. This research demonstrates that A356–fly ash cenosphere composites can be synthesized using gas pressure infiltration technique over a wide range of reinforcement volume fraction from 20 to 65%.
2. The densities of Al356–fly ash cenosphere composites, made under various experimental conditions, are in the range of 1250–2180 kg/m^3 corresponding to the volume fraction of cenospheres in the range 20–65%. The density of composites increased for the same cenosphere volume fraction with increasing melt temperature, applied pressure, and the size of particles. This appears

to be related to a decrease in voids present near particles by an enhancement of the melt flow in a bed of cenospheres.

3. Microstructural observations showed occasional presence of voids in regions where cenospheres were very close to each other. The entrapped void content is around 3% by volume for the highest applied pressure of 275 kPa.
4. The stress–strain curves of composites showed a stress plateau region, which is commonly observed in foam materials when pores are crushed during compression. The composites containing fly ash cenospheres with a density in the range of 1250–2180 kg/m^3 exhibited compressive yield strengths of 9–83 MPa.
5. The compressive strength, plateau stress and modulus of the composites increased with the composite density.

References

[1] Rohatgi PK, Guo RQ, Iksan H, Borchelt EJ, Asthana R. Synthesis of aluminum–fly ash particulate composite by pressure infiltration technique. Mater Sci Eng 1998;A244(1):22–30.

[2] Bader MG, Clyne TW, Cappleman GR, Hubert PA. The fabrication and properties of metal-matrix composites based on aluminium alloy infiltrated alumina fibre preforms. Compos Sci Technol 1985;23(4): 287–301.

[3] Cook AJ, Werner PS. Pressure infiltration casting of metal matrix composites. Mater Sci Eng A 1991;144(1-2):189–206.

[4] Demir A, Altinkok N. Effect of gas pressure infiltration on microstructure and bending strength of porous Al_2O_3/SiC-reinforced aluminium matrix composites. Compos Sci Technol 2004;64(13/14): 2067–74.

[5] Kouzeli M, San Marchi C, Mortensen A. Effect of reaction on the tensile behavior of infiltrated boron carbide–aluminum composites. Mater Sci Eng A 2002;337(1/2):264–73.

[6] Hartmann M, Singer RF. Fabrication and properties of syntactic magnesium foams. In: Schwartz D, Shih D, Evans A, Wadley H, editors. Proceedings of porous and cellular materials for structural applications symposium. Warrendale, PA: Materials Research Society; 1998. p. 211–6.

[7] Hurysz KM, Clark JL, Nagel AR, Hardwicke CU, Lee KJ, Cochran JK, et al. Steel and titanium hollow sphere foams. In: Schwartz D, Shih D, Evans A, Wadley H, editors. Proceedings of porous and cellular materials for structural applications symposium. Warrendale, PA: Materials Research Society; 1998. p. 191–203.

[8] Uslu C, Lee KJ, Sanders Jr H, Cochran Jr JK. Ti–6Al–4V hollow sphere foams. In: Ward-close CM, Froes FH, Chellman PJ, Cho SS, editors. Proceedings of synthesis/processing of lightweight metallic materials II. TMS, 1997. p. 289–300.

[9] Gupta N, Karthikeyan CS, Sankaran S, Kishore. Correlation of processing methodology to the physical and mechanical properties of syntactic foams with and without fibers. Mater Charact 1999;43(4): 271–7.

[10] Gupta N, Kishore, Woldesenbet E, Sankaran S. Studies on compressive failure features in syntactic foam material. J Mater Sci 2001;36(18):4485–91.

[11] Gui MC, Way DB, Yuan JJ, Li CG. Deformation and damping behaviors of foamed Al–Si–SiCp composite. Mater Sci Eng A 2000; 286(2):282–8.

[12] ASM Metals Handbook Desk Edition Online, www.ASTM-Intl.org, Aluminum and Aluminum Alloys; 2001.

[13] Agrawal BD, Broutman LJ. Analysis and performance of fiber composites. 2nd ed. New York: Wiley; 1990.

[14] Mortensen A, Cornie J. On the infiltration of metal matrix composites. Met Trans A 1987;18A:1160–3.

[15] Long S, Zhang Z, Flower HM. Hydrodynamic analysis of liquid infiltration of unidirectional fibre arrays by squeeze casting. Acta Metall Mater 1994;42(4):1389–492.

[16] Gupta N, Brar BS, Woldesenbet E. Effect of filler addition on the compressive and impact properties of glass fiber reinforced epoxies. Bull Mater Sci 2001;24:219–23.

[17] Sobczak N, Sobczak J, Morgiel J, Stobierski L. TEM characterization of the reaction products in aluminium–fly ash couples. Mater Chem Phy 2003;81:296–300.

[18] Balch DK, Dunand DC. Mechanical properties and in situ diffraction strain measurements in aluminum-mullite microsphere syntactic foams produced by liquid metal infiltration. In: Gosh AK, Sanders TH, Claar TD, editors. Proceedings of processing and properties of lightweight cellular metals and structures, TMS third global symposium. Warrendale, PA: TMS; 2002. p. 251–60.

[19] Gupta N, Woldesenbet E. Compression properties of syntactic foams: effect of cenosphere radius ratio and specimen aspect ratio. Composites: Part A 2004;35(1):103–11.

[20] Gibson LJ, Ashby MF.. 2nd ed Cellular solids: structure and properties. vol. 180. Cambridge: Cambridge University Press; 1988.

[21] Matsunuga D. Polymer fly ash composites, MS Thesis; Materials Engineering Department, University of Wisconsin-Milwaukee; 2000.

[22] Palumbo M, Donzella G, Tempesti E, Ferruti P. On the compressive elasticity of epoxy resins filled with hollow glass microspheres. J Appl Polym Sci 1996;60:47–53.

[23] Gupta N, Woldesenbet E. Microballoon wall thickness effects on properties of syntactic foams. J Cell Plast 2004;40(6):461–80.

[24] Nagal AR, Uslu C, Lee KJ, Cochran JK, Sanders Jr. TH. Steel closed cell foams from direct oxide reduction. In: Ward-Close CM, Froes FH, Chellman DJ, Cho SS, editors. Proceedings of synthesis/processing of lightweight metallic materials II. Warrendale, PA: TMS; 1997. p. 395–406.

[25] Huang JS, Gibson LJ. Fracture toughness of brittle honeycombs. Acta Metall Mater 1991;37(7):1617–26.

[26] Triantafillou TC, Gibson LJ. Failure mode maps for foam-core sandwich beams. Mater Sci Eng 1987;95:37–53.

[27] Thornton PH, Magee CL. Deformation characteristics of zinc foam. Phy Met Mater Sci 1975;6A(9):1801–7.